The Ara OB1 Association and its Molecular Complex

E. M. Arnal

Instituto Argentino de Radioastronomía, C.C. 5, Villa Elisa 1894, Argentina and Facultad de Cs. Astronómicas y Geofísicas, UNLP, Paseo del Bosque S/N, 1900, La Plata, Argentina

G. A. Romero

Instituto Argentino de Radioastronomía, C.C. 5, Villa Elisa 1894, Argentina

J. May

Departamento de Astronomía, Universidad de Chile, Casilla 36-D, Santiago, Chile

D. Minniti

Department of Astronomy, Pontificia Universidad Católica, Casilla 306, Santiago 22, Chile

Abstract. The results of low (HPBW[1]=8′.7) and intermediate (HPBW=2′.7) angular resolution carbon monoxide (^{12}CO $J= 1 \rightarrow 0$) line observations toward the OB association Ara OB1 are reported. The molecular features that are likely to be associated with the OB-association span a velocity range from -28 to -20 $km\,s^{-1}$. The most negative radial velocities are observed along NGC 6188 (also known as the Rim Nebula). The main CO structures, labeled E and F in Fig. 2, have radial velocities of about -23.5 and -21.8 $km\,s^{-1}$, respectively. The former harbors the IRAS source IRAS 16362−4845 and the infrared cluster RCW 108-IR. The observations at intermediate resolution show noticeable changes in shape, peak intensity and full width at half maximum in the line profiles observed toward structures E and F. The large line widths, about 7.5 $km\,s^{-1}$, found toward structure E very likely reflect the interaction of RCW 108-IR with its surrounding molecular gas. A scale down version of this phenomenon is also found toward structure F. The total amount of molecular gas related to structures E and F in NGC 6188 is about $8.2 \times 10^3\,M_\odot$.

Introduction

Ara OB1 is an OB association in the southern sky (l=336°.5, b=-1°.5). It has an age of $\sim 5 \times 10^6$ yr (Whiteoak 1963) and covers an area of ~ 1 square degree around its central cluster NGC 6193. The most massive members of this cluster, the stars HD 150135 and HD 150136, are the main ionizing sources of the low surface brightness optical emission nebula RCW 108 (Rodgers, Campbell &

---

[1]Half Power Beam Width

Whiteoak 1960). About 15′ westwards of these stars, we find the Rim Nebula (also known as NGC 6188), which marks the interface between RCW 108 and a nearby dense dark nebula. Herbst & Havlen (1977) derived a distance of 1320±120 pc to this cluster (see Arnal, May & Romero 2003, for a brief discussion).

The average barycentric radial velocity[2] of NGC 6193 is $-30.0 \pm 2.8\,\mathrm{km\,s^{-1}}$ (Arnal et al. 1988), while the radial velocity of RCW 108 is about $-20\,\mathrm{km\,s^{-1}}$ (Georgelin & Georgelin 1970; Cersósimo 1982; Georgelin et al. 1996).

Westwards of NGC 6193, embedded in a dark cloud, there is an R association called Ara R1 (Herbst 1975), a bright optical knot (Frogel & Persson 1974) and a compact young infrared cluster (RCW 108-IR) (Straw et al 1987).

High resolution radio continuum observations at 5 GHz (Goss & Shaver 1970) detected a small, high emission measure compact H II region that might be powered by an O8-O9 main sequence star (Urquhart et al. 2004). Radio recombination line observations of this source (Wilson et al. 1970; Caswell & Haynes 1987) provide a radial velocity of about $-25\,\mathrm{km\,s^{-1}}$, which is in very good agreement with single-pointing molecular line observations carried out toward RCW 108-IR (see Arnal et al. 2003 and references therein). Recently, a small area ($2' \times 2'$) centred on IRAS 16362−4845 has been surveyed by Urquhart et al. (2004), whilst a more extended area (roughly a square region 20′ in size) covering NGC 6193, part of NGC 6188 and IRAS 16362−4845 has been studied by Comerón, Schneider & Russeil (2005). Arnal, May & Romero (2003) mapped a $2°.75 \times 3°.00$ region around RCW 108 at 8′.7 resolution in the 115 GHz CO line.

Herbst & Havlen (1977) suggested that the formation of Ara OB1 may have been triggered by a supernova explosion, while Arnal et al. (1987) suggested that NGC 6193 was formed by the action of an expanding H I shell that is possibly generated by the winds of the massive stars in NGC 6167.

For the reader's benefit and the sake of clarity the main optical constituents and their relative locations are superimposed on a R-band MAMA image of the Ara OB1 region (see Fig. 1)

Observations and Data Reduction

The $^{12}\mathrm{CO}$ ($J= 1 \rightarrow 0$) line observations were carried out with the 1.2m Columbia University telescope at CTIO (November 1996) and the 4m NANTEN telescope at LCO (May 2001). Data taken with the former (latter) have a resolution of 8′.7 (2′.7), a velocity resolution of 0.26 (0.055) km s^{-1} and a RMS noise level of 0.15 (0.35) K.

Results

Using the data collected at CTIO and relying on morphological and kinematical criteria, nine molecular concentrations were found to be associated with Ara OB1. These features constitute what we call the Ara OB1 molecular complex. Five of these structures are shown in Fig. 2. This figure shows the in-

---

[2]All velocities in this paper are referred to the Local Standard of Rest (LSR)
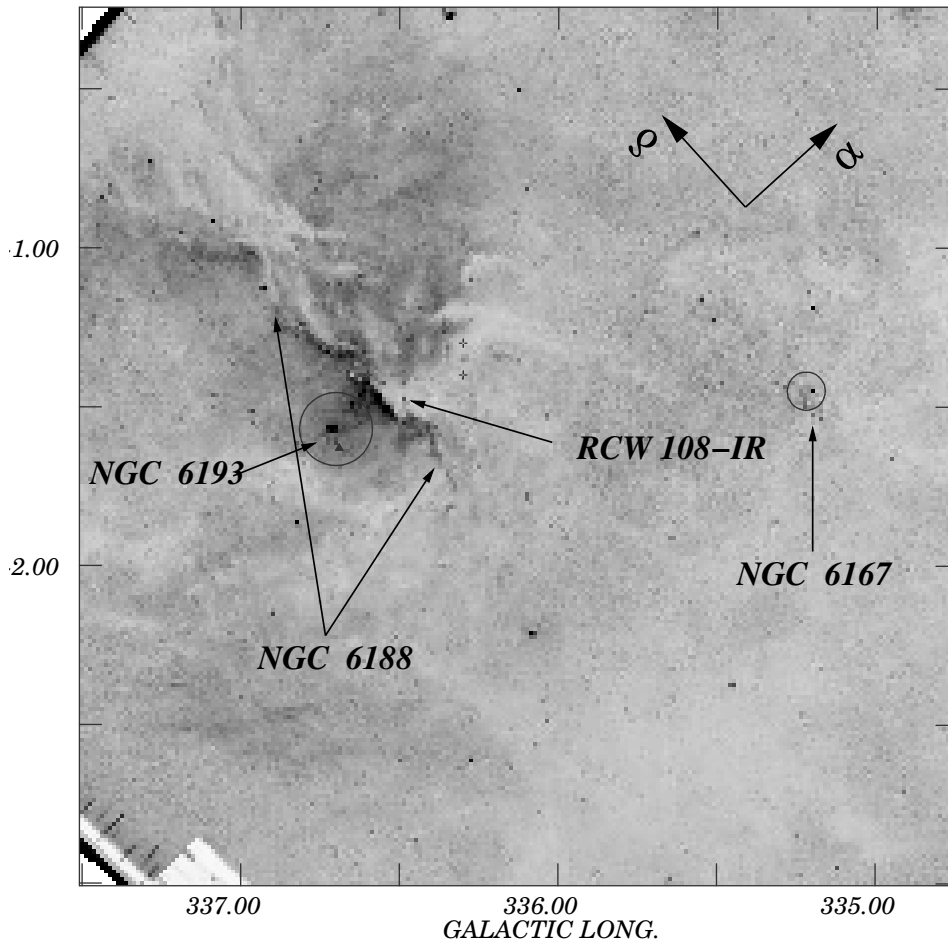
Figure 1.   Gray scale MAMA R-band image of the Ara OB1 region. The diameters of the circles correspond to the optical diameters of the open clusters NGC 6193 and NGC 6167. The filled triangle within the circle defining the location of NGC 6193 marks the region observed by Phillips et al. (1986). The plus signs indicate the position of some members of Ara R1 (Herbst 1975). Single-pointing molecular line observations were mostly taken at the position of RCW 108-IR. An indication of the orientation of the equatorial coordinate system is provided by the arrows in the upper right corner.

tegrated CO emission (contour lines) in the velocity range -27 to -23 km s^{-1} overlaid on an Hα image (grey scale). Features B and D very likely trace the molecular gas related to NGC 6188, whilst feature E marks the location of the infrared cluster RCW 108-IR. The IRAS point source IRAS 16362−4845 is the far infrared counterpart of the infrared cluster discovered by Straw et al (1987). The IRAS source IRAS 16348−4849 is seen projected onto feature F. Their radial velocities lie in the range -24 to -23.5 km s^{-1} . Their masses, ∼4000 M$_\odot$ for E and ∼3000 M$_\odot$ for F, were derived using the relationship between the H$_2$

column density ($N(H_2)$) and the equivalent width of CO (W_{CO}) given by Strong et al. (1988), namely $(N(H_2)/W_{CO})=(2.3\pm0.3)\times10^{20}$ mol. cm^{-2}.
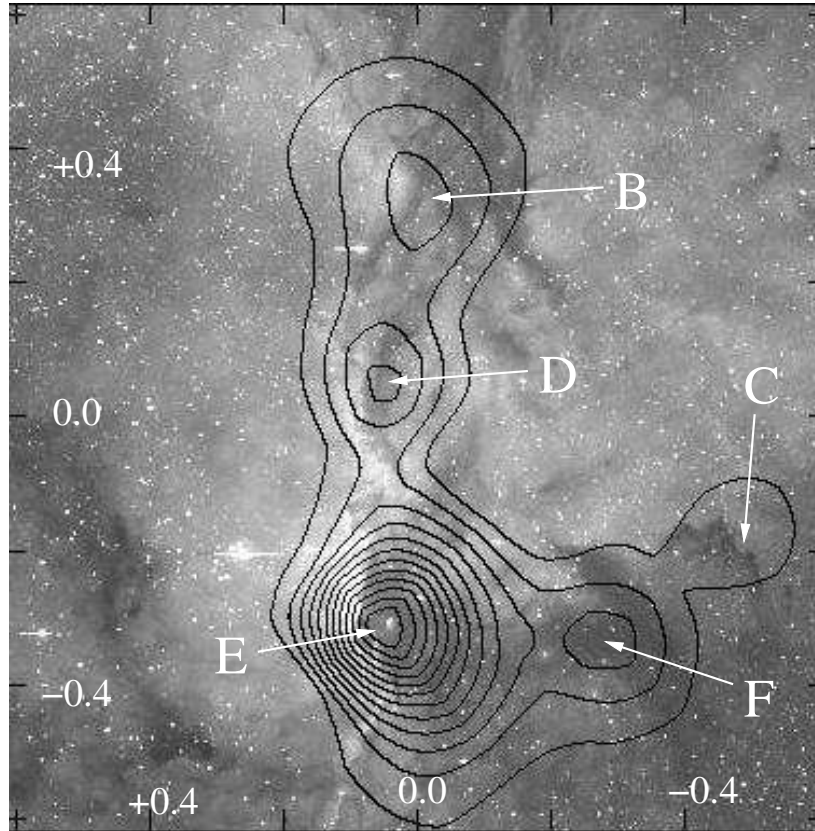

Figure 2.   Overlay of the integrated CO distribution (contours between -27 and -23 km s^{-1}) from the observations made at CTIO on an Hα image (grey scale). The ordinate and the abscissa are angular offsets (in degrees) from the reference position (α, δ)(1950.0)=(249°00, -48°46)

The higher angular resolution of the NANTEN data allows us to study in some detail the kinematical behavior of individual CO features. Fig. 3 shows average carbon monoxide profiles obtained toward different regions of concentration E. The changes in shape, peak intensity and full-width at half maximum among the different profiles *of the same concentration* are easily noticeable. The strongest (~22 K) and broadest (~7 km s^{-1}) lines are observed toward IRAS 16362−4845. The kinematics may reflect the interaction between the infrared cluster RCW 108-IR and its surrounding molecular gas.

The NANTEN data also revealed a radial velocity gradient of -0.25 km s^{-1}pc^{-1} along NGC 6188. The radial velocity decreases from north to south.
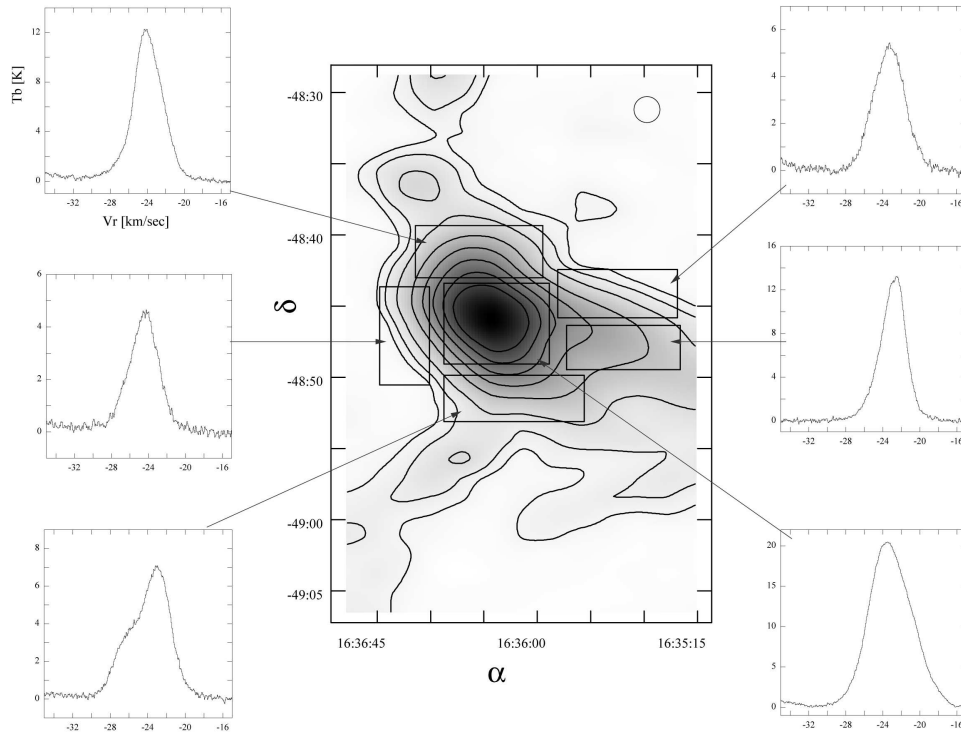
Figure 3.   Representative sample of average CO profiles obtained towards different regions of feature E. The profile units are T_A^* in K (ordinate) and V_{LSR} in $km\,s^{-1}$ (abscissa).

References

Arnal, E. M., Cersósimo, J. C., May, J., & Bronfman, L. 1987, A&A, 174, 78

Arnal, E. M., Morrel, N. I., García, B., & Levato, O. H. 1988, PASP, 100, 1076

Arnal, E. M., May, J. & Romero, G. A. 2003, A&A, 412, 431

Caswell, J. L., & Haynes, R.F. 1987, A&A, 171, 261

Cersósimo, J. C. 1982, ApJL, 22, 157

Comerón, F., Schneider, N. & Russeil, D. 2005, A&A, in press (astro-ph/0412125)

Frogel, J. A., & Persson, S. E. 1974, ApJ, 214, 725

Georgelin, Y. P., & Georgelin, Y. M. 1970, A&A, 6, 349

Georgelin, Y. M., Russeil, D., Marcelin, M., Amram, D., Georgelin, Y. P., Goldés, G., le Coarer, E., & Morandini, M. 1996, A&AS, 120, 41

Goss, W. M., & Shaver, P.A. 1970, Australian J. Phys., Ap. Suppl. 14, 1

Herbst, W. 1975, AJ, 80, 212

Herbst, W., & Havlen, R.J 1977, A&AS, 30, 279

Phillips, J. P., de Vries, C. P., & de Graauw, T. 1986, A&AS, 65, 465

Rodgers, A. W., Campbell, C. T., & Whiteoak, J.B. 1960, MNRAS 121, 103

Straw, S., Hyland, A. R., Jones, T. J., Harvey, P. M., et al. 1987, ApJ, 314, 283

Strong, A. W., Bloemen, J. B. G. M., Dame, T. M., Grenier, I.A., Hermsen, W., Lebrun, F., Nyman, L.-Å, Pollock, A. M. T., & Thaddeus, P. 1988, A&A, 207, 1

Urquhart, J. S., Thompson, M. A., Morgan, L. K. & White, G. J. 2004, A&A, 428, 723

Whiteoak, J. B. 1963, MNRAS, 125, 105

Wilson, T. L., Mezger, P. G., Gardner, F. F., & Milne, D. K. 1970, A&A, 6, 364
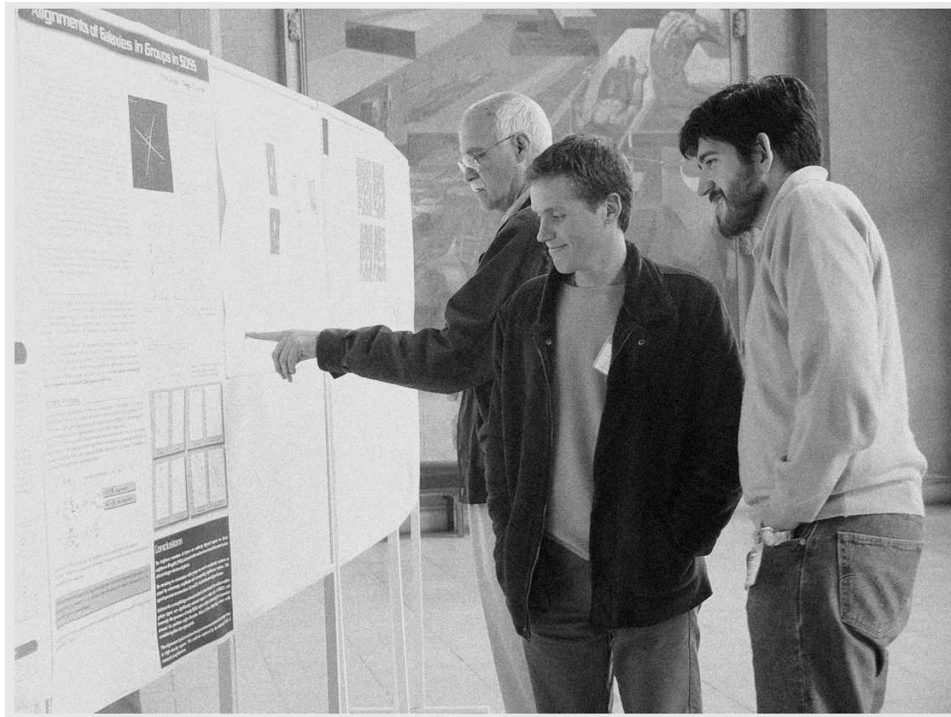
E. Arnal (left) reading one of the posters.